Theory of the formation of metallic glasses

J. Hafner

*Max-Planck-Institut für Festkörperforschung, Heisenbergstrasse 1, D 7000 Stuttgart 80, Germany and Institut für Theoretische Physik, Technische Universität Wien, Karlsplatz 13, A 1040 Wien, Austria**

(Received 7 September 1979)

The structure and stability of metallic glasses and the relationship between the constitution diagram and glass formation in binary alloy systems is discussed on a quantum-mechanical basis. An *ab initio* pseudopotential method is used to calculate the interatomic forces in transition-metal-free glass-forming alloys. The knowledge of the interatomic forces allows a microscopic calculation of the structure and of the thermodynamic properties of the crystalline, liquid, and amorphous intermetallic phases. The liquid and amorphous structures are calculated using cluster-relaxation and thermodynamic variational techniques. We show that the bonding in all stable phases arises from an optimal embedding of the neighboring atoms into the attractive minima of the interatomic pair potentials—for disordered phases this is visualized by the close matching between the minima in the pair potentials and the maxima in the partial pair-distribution functions. The role of the traditional alloy-chemical factors [(i) size ratio, (ii) strong chemical bonding (charge transfer and screening), and (iii) valence-electron concentration] in establishing this "constructive interference" is elucidated. It is argued that the geometrical basis of all these structures—crystalline as well as disordered—is tetrahedral close packing. For a majority concentration of the smaller atoms this leads to Frank-Kasper phases; for a majority concentration of the larger atoms this leads to a random tetrahedral packing based on icosahedral microunits. Thus the interrelation between the formation of topologically close-packed intermetallic compounds, the formation of eutectic phase diagrams, and the formation of metallic glasses is readily, and quantitatively, understood. The use of the pseudopotential technique restricts the application of our method to simple-metal glasses, but we argue that many of our results apply to all metalloid-free metallic glasses.

I. INTRODUCTION

Since the early work of Klement, Willens, and Duwez[1] on the rapid solidification of liquid metals, a large number of alloys has been prepared as metallic glasses. It is now widely believed that nearly all metallic liquids would undergo a transition to a glassy state provided that crystallization could be bypassed. Whether or not a glass forms at a given cooling rate depends on thermodynamic conditions that favor the disordered (liquid or amorphous) relative to the crystalline state and on kinetic conditions that inhibit crystallization. In this paper we shall concentrate on the first point. We want to explore the microscopic origin of the interatomic forces that yield a relatively low free energy for a disordered atomic arrangement in some systems, while for other systems a periodic structure is strongly preferred.

Several models have been proposed to explain the relative stability of metallic glasses. They are all based on the observation that glass formation occurs most easily in systems possessing a deep eutectic minimum in the phase diagram and is usually restricted to a quite narrow concentration region around the eutectic. The existence of a deep eutectic may be related either to a very high stability of the liquid relative to the crystalline solid phase or to a destabilization of the crystalline mixture. The stabilization of the liquid has been related to packing effects or electronic effects. Bennett and co-workers[2] suggested that the smaller and softer metalloid atoms in transition metal-metalloid glasses (e.g., $Pd_{1-x}Si_x$, $Fe_{1-x}B_x$, $\times 0.15-0.25$) fill the large holes in a dense random packing of hard spheres (DRPHS). From the size and number of these holes one might predict a concentration of just 15 to 25 % metalloid atoms, in good agreement with some of the classical glass-forming metal-metalloid alloys. However, this model is unable to explain the stability of amorphous metal-metal alloys. Nagel and Tauc[3] used a free-electron type argument and argued that for $Q = 2k_F$, where k_F is the Fermi wave vector and Q the wave vector of the first peak in the static structure factor $S(q)$, the Fermi level falls into a minimum in the electronic density of states. Thus the disordered state should have a relatively low electronic energy. Nagel and Tauc's argument is built in analogy to the Mott-Jones formulation of the Hume-Rothery rules for crystalline alloys. Hume-Rothery's critical valence-electron concentrations (VEC's) correspond to the case of a Jones-zone plane touching the Fermi sphere, i.e., $|\vec{Q}| = 2k_F$ where $\vec{Q}$ is now a vector of the wavenumber lattice. In this case a gap opens in the energy band at $\frac{1}{2}\vec{Q}$ and produces a minimum in the density of states. Of course there are no bands and consequently no band gaps in the disordered state, but Nagel and Tauc proposed that

there should be a "pseudogap" which is manifested through a minimum in the density of states. This pseudogap must be isotropic and should lower the electronic energy of the amorphous structure relative to a crystalline structure with anisotropically distributed gaps. If k_F is estimated in a free-electron approximation (and the d electrons are ignored in the count) the condition $Q = 2k_F$ is indeed met for a number of metallic glasses. The conjecture gains further support from the fact for $Q = 2k_F$ a straightforward extension of the Faber-Ziman theory[4-6] for the electronic transport properties of liquid metals explains the negative temperature coefficient of the electrical resistivity found in many amorphous systems. However, recent photoemission experiments[7,8] failed to confirm the predominantly s-like character of the electronic states near the Fermi level of $Pd_{80}Si_{20}$ postulated by Nagel and Tauc and low-temperature specific-heat measurements[9] on amorphous Pd-Si-Cu and Pd-Si alloys failed to confirm the minimum in the density of states at E_F. Esposito *et al.*[10] have criticized the use of the Faber-Ziman theory for systems containing strong-scattering transition-metal ions. In the free-electron limit, the Nagel-Tauc theory reduces to a VEC rule predicting optimum glass formation for a VEC $\simeq 2$ e/at. Giessen and co-workers[11] have pointed out that among the Ca-based metallic glasses, those with Mg and Zn (average VEC = 2.0) are the least stable ones, whereas those with Al and Ga (VEC $\simeq 2.4$) and Cu, Ag, and Au (VEC $\simeq 1.6$) are much more stable. Hence the Nagel-Tauc rule, though still an interesting conjecture, is far from being universally accepted.

On the other side, Chen[12] proposed that the destabilization of the crystalline mixture rather than the stabilization of the liquid near the eutectic composition is responsible for the easiness of glass formation. Chemical affinity stabilizes stoichiometric crystalline AB_5, AB_2... phases (cf. below). The destabilization of the crystalline phases with higher A concentrations is thought to be due to the mismatched energy arising from the addition of atoms of different size to the crystalline phases and would explain the observed eutectic compositions of 20–30% B atoms. This parallels a conjecture of Turnbull[13] that there might be alloy compositions for which the free enthalpy of the amorphous solid is lower than that of any *single* crystalline phase. In that case a glass must be formed if the alloy is constrained against crystallization in a two-phase mixture.

Giessen and co-workers[14,15] pointed out that there is a remarkable coincidence between glass formation and the formation of certain classes of stoichiometric compounds such as Frank-Kasper[16] phases (Laves, μ, and σ phases) and cementite (Fe_3C)-type phases. It is certainly worthwhile to pursue this correlation somewhat further. In Table I we present a classification of binary glass-forming systems according to the chemical nature of their components: simple metals (S), transition metals (T), rare-earth metals (R), and metalloids (M). It is evident that the metallic glasses may be grouped in three main classes: (a) The now classical T-M glasses of the Pd-Si type.[17] They are characterized by the simultaneous occurrence of cementite-type crystalline compounds, the chemical bonding in these systems is at least of partially covalent character. In the remaining classes there is no evidence for any nonmetallic contribution to the bonding forces. The S-S,[18] S-T,[19] and T-R (Ref. 20) glasses may be grouped under a common heading. (b) They are characterized by the formation of highly stable (congruently melting) AB_2 Laves phases or closely related Frank-Kasper structures ($CaCu_5$, Th_2Mn_{17}, $BaCd_{11}$, $NaZn_{13}$ types, etc.) at majority concentrations of the smaller B atoms. Glasses are formed at a majority concentration of the larger A atoms. In this region of the phase diagram there are no, or only relatively unstable (peritectically decomposing), crystalline intermetallic compounds. Some prototype phase diagrams are depicted in Figs. 1(a) to 1(c). There appears to be a clear correlation between the width of the glass-forming region and the stoichiometry of the stablest intermetallic compound (the one with the highest melting point; this correlation will be explained in more detail later on). We shall designate this group of metallic glasses as "anti-Laves phases," a term which has been proposed by Giessen[15] for the Ca-based amorphous alloys. The third group (c) contains the metallic glasses formed by transition metals only.[22] This class is characterized by complex tetrahedrally close-packed structures of the Frank-Kasper type, such as the μ and σ phases. Contrary to the anti-Laves phases, the glass-forming region overlaps with the usually rather broad homogeneity range of the crystalline compounds; a typical phase diagram is shown in Fig. 1(d). While the crystalline phases belonging to group (b) are usually strictly ordered and characterized by a size ratio $r_A/r_B \geq 1.15$, the phases of group (c) show a tendency towards substitutional disorder with a size ratio $r_A/r_B \leq 1.15$.

In this paper we shall demonstrate that it is now possible to explain the constitution diagrams and the interrelation between glass formation and phase diagram from a microscopic quantum-mechanical basis. To begin with, let us sketch the path to be followed for an *ab initio* calculation of a phase diagram:

TABLE I. Classification of glass-forming binary metallic systems according to the chemical nature of their components.

Class [a]	Glasses (typical composition)	Characteristic (most stable) intermetallic compounds	
T-M	$Pd_{80}Si_{20}$	Pd_3Si, Fe_3P (cementite)	group (a)
	$Fe_{80}P_{20}$	Pd_2Si, Fe_2P	
S-S	$Mg_{70}Zn_{30}$	$MgZn_2$ } Laves phases	
	$Ca_{67}Mg_{33}$	$CaMg_2$ }	
	$Ca_{67}Al_{33}$	$CaAl_2$ }	
	$Ca_{60}Zn_{40}$	$CaZn_2$, $CaZn_{11}$, $CaZn_5$	
S-T	$Ca_{65}Pd_{35}$	$CaPd_2$ Laves phase	
	$Ca_{65}Cu_{35}$	$CaCu_5$ } Frank-Kasper phases	
	$Ti_{60}Be_{40}$	Ti_2Be_{17} }	group (b)
		$TiBe_2$ Laves phase	
S-R	$La_{70}Al_{30}$	$LaAl_2$ } Laves phases	
	$Ce_{70}Al_{30}$	$CeAl_2$ }	
T-R	$Gd_{67}Co_{33}$	$GdCo_2$ Laves phase	
		$GdCo_5$ } Frank-Kasper phases	
		Gd_2Co_{17} }	
T-T	$Nb_{60}Ni_{40}$	"NbNi" } disordered μ phases	
	$Ta_{60}Ni_{40}$	"TaNi" }	
	$Fe_{55}W_{45}$	Fe_7W_6 μ phase	group (c)
	$Ta_{55}Ir_{45}$	σ phases with 60–80% Ta	
	$Ta_{55}Rh_{45}$		

[a] S—simple metal; T—transition metal; R—rare-earth metal; M—metalloid.

(1) Calculate the self-consistent atomic potentials of the components. (2) Assume composition (concentration). (3) Assume possible crystal structure. (4) Assume lattice constants. (5) Superpose atomic potentials, calculate self-consistent band structure and electronic total energy. (6) Repeat (5) for different values of the lattice constants to determine their equilibrium values.

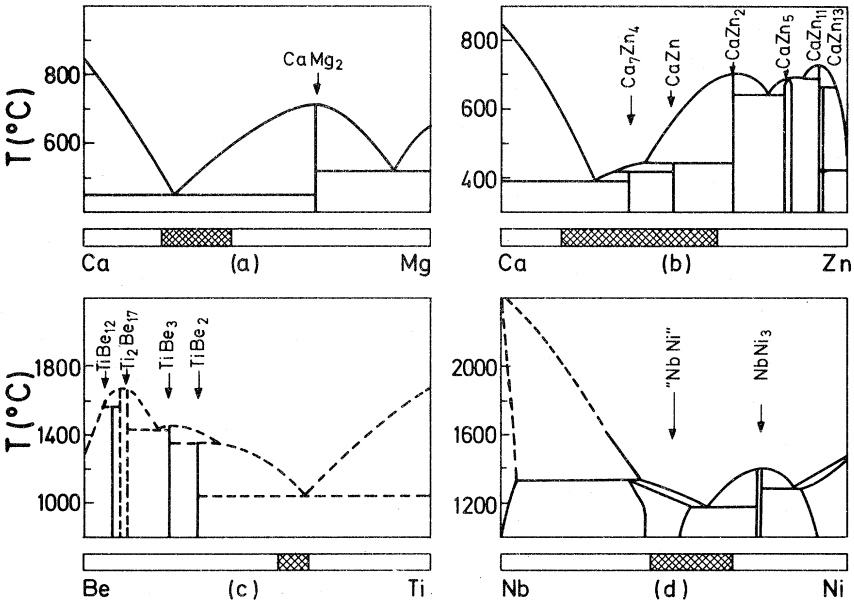

FIG. 1. Typical phase diagram of glass-forming systems (after Ref. 21, cf. text).

(7) Repeat (4) to (6) for other possible structures. (8) Repeat (2) to (7) for other concentrations. As a final result of this procedure we obtain the enthalpies of the possible alloy phases at $T = 0$ K and at a given pressure as a function of concentration. The stable phases and the boundaries of their homogeneity ranges are given by the well-known common-tangent construction. Beyond the determination of the stable phases we can get at least an indication on the possible formation of metastable phases, e.g., if the system is constrained against phase separation.[30] The procedure given above is restricted to $T = 0$ K; for finite temperatures we have to add the thermal entropy which is the sum of a vibrational and a configurational part. In principle this necessitates a complete knowledge of the vibrational and the defect structure of the crystal. For configurationally disordered systems there is an additional complication: Starting with an initial guess for the interatomic forces, we have to calculate the atomic structure. For this atomic structure, we have to calculate the electronic structure. This gives an improved estimate for the interatomic forces and the whole cycle has to be iterated to self-consistency. It is quite clear that in general the realization of this program is a tremendous computational task. However, for simple metals pseudopotential theory allows some substantial simplifications.[23,24] Within second-order perturbation theory and linear screening, the interatomic forces are simply central pair potentials and volume forces, and the problem of the total energy calculation is reduced to the computation of lattice sums (in either direct or reciprocal space) over the structure-independent effective interatomic pair potentials. The construction of appropriate interatomic potentials for binary alloys is described in Sec. II. In Sec. III we apply these potentials to calculate the ground-state properties (relative structural energies, enthalpy, and volume of formation) of crystalline intermetallic compounds and solid solutions in some glass-forming simple metal alloys (Mg-Zn, Ca-Mg, Ca-Al, Ca-Zn). We show that the formation of close-packed Frank-Kasper phases[16] may be understood in terms of a pair-potential picture. Once the interatomic forces are known, the atomic structure of the disordered (liquid or amorphous) phases may be calculated either using a fully numerical procedure (molecular dynamics, Monte Carlo, or cluster relaxation) or using one of the thermodynamic perturbation theories [Gibbs-Bogolyubov variation method[25,26] or Weeks-Chandler-Anderson (WCA) method].[27] The results for the liquid-state structural and thermodynamic properties obtained by the variation method are presented in Sec. IV. The results of a cluster-relaxation calculation for a glassy $Mg_{0.7}Zn_{0.3}$ alloy[28] are discussed in Sec. V. We show that within the pair-potential approach, the structure of the amorphous alloy may be interpreted in a way which is very similar to the interpretation of the Laves-phase $MgZn_2$. Moreover we show that a supercooled liquid, described by the Gibbs-Bogolyubov method is a very good first approximation to the structure of the glass. This allows for the extension of the correlation between the pair potentials and glass formation to a number of other interesting systems. In Sec. VI we combine the results of the three preceding sections in order to derive the principal features of the phase diagram from our *ab initio* calculations. This allows for the elucidation of the interrelation between the phase diagram and glass formation on one side and between the stability of Frank-Kasper phases and glass formation on the other side. Technically, the application of our methods is restricted to transition-metal-free systems. However, we think that most of our results apply to transition metals too, the main problem being to find an appropriate way to define interatomic pair potentials.

Some of our results have been announced recently in the form of a short letter.[29]

II. INTERATOMIC FORCES IN BINARY ALLOYS

Pseudopotential methods have been very successful in describing the physical properties of many pure simple metals.[23,24] The application of the scheme to alloys was at first somewhat less successful. This is related to the fact that the pseudopotential is often considered as a purely atomic property which is (except for conduction electron screening effects) independent of the atom's surrounding. In reality the pseudopotential is a collective rather than an atomic property. It describes the *scattering of electrons by an atom in a given effective medium* (the average potential of all other ions and electrons in the crystal). If this effective medium changes (e.g., by alloying), the pseudopotential changes too. It might be difficult to imagine how such effects could be incorporated in a parametrized model-potential theory, but they appear in a very natural fashion in an *ab initio* pseudopotential theory based on orthogonalized plane waves (OPW's).[30] In an A-B alloy we have to orthogonalize the conduction-electron states to two different sets of core states, those of the A and B ions. This is the starting point for the derivation of an optimized alloy pseudopotential which is a straightforward generalization of Harrison's pure metal theory.[23]

The remaining ingredients of the method are a local-density approximation for the core-core and the core-valence electron exchange and correlation[31] and the use of the Vashishta-Singwi approach[32] for many-body effects in the conduction-electron screening function. The method is well documented in several papers,[26,30,33] only a few points should be made here: The pseudopotential form factors w_A, w_B of the components in the alloy depend on the alloy partner and on the concentration, and they are different from those of the pure metals, even recalculated at the atomic volume and screened by the valence electron density of the alloy. The core electron eigenvalues are modified due to the presence of the second component; this changes the strength of the repulsive parts of the pseudopotentials w_A and w_B. The orthogonalization of the valence states is equivalent to push the conduction electrons out of the core region each ion "digs an orthogonalization hole."[23] If we alloy two components with appreciably different valence electron densities, e.g., Ca (atomic volume $\Omega = 43.50$ Å^3, valence $Z = 2$, electron density $Z/\Omega = 0.046\ e/$Å^3) and Al ($\Omega = 16.51$ Å^3, $Z = 3$, $Z/\Omega = 0.182\ e/$Å^3), the one which feels a higher electron density must dig a bigger orthogonalization hole, while around the other ion it is reduced. The orthogonalization hole of Ca increases from 0.353 e/at. in the pure metal to 0.835 e/at. in a $CaAl_2$ alloy, the Al-orthogonalization hole is reduced from 0.241 e/at. to 0.161 e/at. The charge neutrality of the pseudoatoms requires the screening charges to compensate for the change in the effective valences (effective valence $Z^* =$ normal valence $Z +$ orthogonalization hole). In order to maintain the charge neutrality even on a local level, the additional screening charge of the Ca pseudoatom is accumulated in the core region [Fig. 2(a)]. This is accompanied by an inward shift of the Friedel oscillations in the screening charge distribution. Around the Al ion the effect goes into the other direction: depletion of the screening charge in the core, outward shift of the Friedel oscillations. The interaction between two pseudoatoms is described by the effective interatomic potential. On alloy-

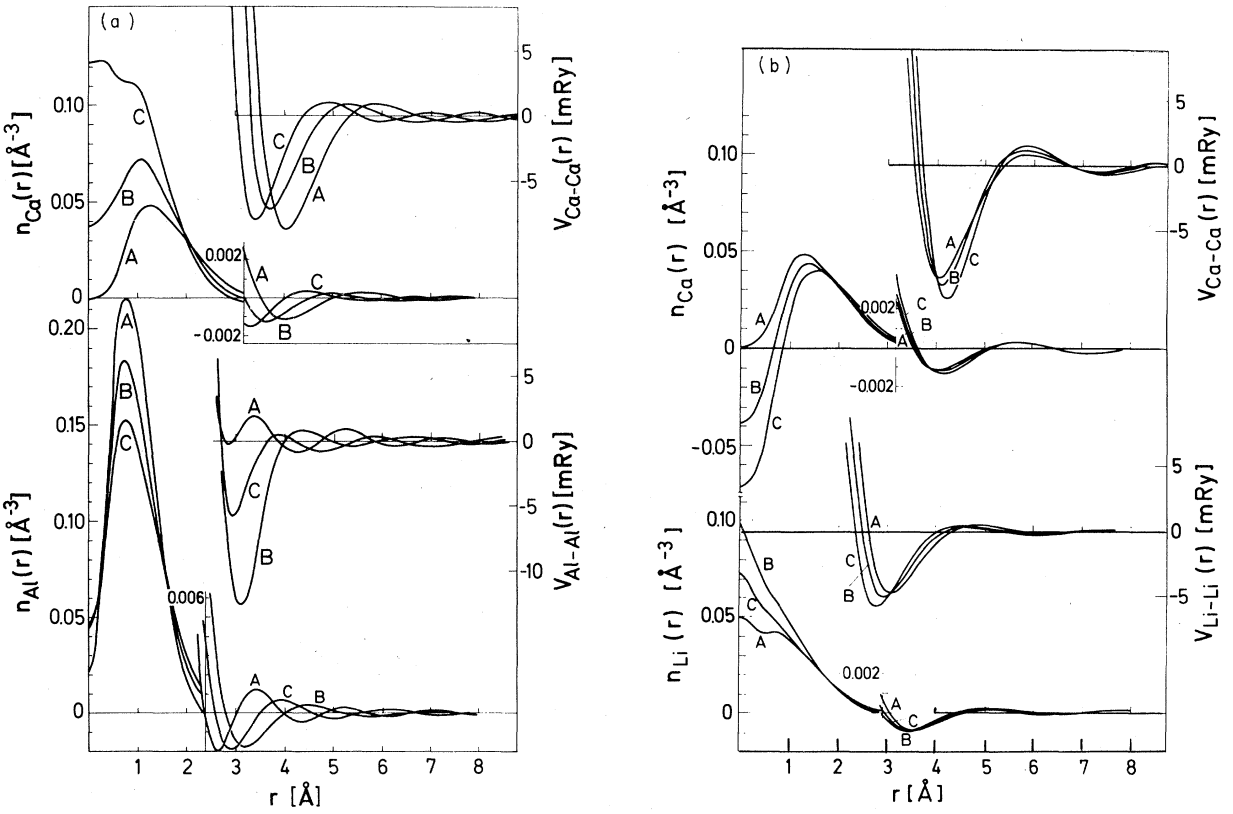

FIG. 2. Pseudoatom (screening) charge density $n_i(r)$ and effective interatomic pair potentials $V_{ij}(r)$ for (a) Ca and Al atoms and (b) Ca and Li atoms in the pure metals (curve A) and in alloys of the compositions $Ca_{0.67}X_{0.33}$ (curve B) and $Ca_{0.33}X_{0.67}$, $X =$ Al, Li, demonstrating the "chemical compression" of the electropositive atom in the alloy.

ing, the interatomic potentials follow very closely the redistribution of the screening charges. The change in the short-range part of the potentials is equivalent to a shrinking of the Ca ion and an expansion of the Al ion. This is a microscopic explanation for an effect which is well-known in the metallurgical literature as the "chemical compression"[34] of an electropositive atom on alloying with a more electronegative atom. If Ca is alloyed with a still more electropositive metal, e.g., with Li, the effect goes into the other direction: The screening charge is accumulated at the site of the Li ion and reduced around the Ca ion; the effective diameter of the Li atom shrinks, while the Ca pseudoatom is slightly expanded [Fig. 2(b)]. Our results corroborate Pauling's[35] early discussion of the role of electron transfer effects in intermetallic compounds. We assume that the B component in an A-B alloy is more electronegative than A. Thus the bonding in the alloy has some ionic character, A has a positive and B a negative charge. This corresponds to the orthogonalization part of our calculation (we refer also to the interrelation between effective charges and electronegativity as discussed by Hafner and Sommer[36]). According to the electroneutrality principle, the stability of the compound is increased if the charges in the atomic cells are reduced by a transfer of electrons from B to A. This corresponds to the screening part of our calculation. It is remarkable that electrons are transferred to the electropositive component—thus in the opposite direction as in the formation of ions in ionic compounds. The effects discussed here exist in all alloys, but they are certainly more important in alloys with large differences in the electronic density and in the electronegativity of both components. A very clear example of their importance will be given at the example of the series of $CaAl_2$, $CaMg_2$, $CaLi_2$, Laves phases.

It is interesting to note that the position of the first minimum in the pair potential of the pure metals $2R_{\min}$ agrees very well with the interatomic distance in a close-packed structure (= two times the Goldschmidt radius R_M, the metallic radius for twelvefold coordination); Ca: $R_{\min} = 2.03$ Å, $R_M = 1.97$ Å; Mg: $R_{\min} = 1.59$ Å, $R_M = 1.60$ Å; Zn: $R_{\min} = 1.42$ Å, $R_M = 1.34$ Å; Li: $R_{\min} = 1.61$ Å, $R_M = 1.56$ Å; Al: $R_{\min} = 1.43$ Å, $R_M = 1.45$ Å. This suggest that the radius $R_{\min}$ (which varies on alloying) is a more sensible measure of the effective atomic size than the rigid radius R_M.

The configurational (structure-dependent) part of the internal energy per atom of the crystalline alloy is given by the sums[30,33] ($\sum_{i(A)}$ and $\sum_{i(B)}$ extend over the A and B sublattice, respectively N is the number of atoms in the crystal)

$$E_{st} = \frac{1}{2N} \sum_{i(A)} \sum_{j(A)}{}' V_{AA}(|\vec{r}_i - \vec{r}_j|) + \sum_{i(B)} \sum_{j(B)}{}' V_{BB}(|\vec{r}_i - \vec{r}_j|) + \sum_{i(A)} \sum_{j(B)} V_{AB}(|\vec{r}_i - \vec{r}_j|) . \quad (1)$$

Using the partial pair-distribution functions $g_{lm}(r)$, we can write the configuration energy of an amorphous or liquid phase as (c_A and c_B are the concentrations of the A and B atoms)

$$E_{st} = 4\pi \left\{ c_A^2 \int V_{AA}(r)[g_{AA}(r) - 1] r^2 dr + c_B^2 \int V_{BB}(r)[g_{BB}(r) - 1] r^2 dr + 2c_A c_B \int V_{AB}(r)[g_{AB}(r) - 1] r^2 dr \right\} . \quad (2)$$

Equations (1) and (2) allow an interpretation of the structural stability in terms of pair interactions and a first estimate of the structural energies. For an exact calculation of E_{st}, a reciprocal space representation is preferable.[30,33]

III. CRYSTALLINE ALLOYS

A. Tetrahedrally close-packed Frank-Kasper phases and related structures

In the introduction we have pointed out that the constitution diagrams of many glass-forming systems are characterized by the occurrence of tetrahedrally close-packed intermetallic compounds of the Frank-Kasper type. In a recent paper we have shown that the formation of Frank-Kasper phases in binary alkali-metal systems (Na_2K, Na_2Cs, K_2Cs-hexagonal Laves phases,[37] K_7Cs_6-hexagonal stacking variant of a μ phase[38]) may be explained by pseudopotential theory in terms of an energetically very favorable packing of a large number of atoms (high coordination numbers) into the minima of the interatomic pair potentials. As the first microscopic treatment of such complex structures the theory was certainly a success, though it must be admitted that from the nature of the constituent metals—the alloys are homovalent and thus electronic effects are present, but rather small—the problem was still quite simple. The formation of Laves phases of Ca with Al, Mg, and Li (the first two systems form glasses, while the last one does not) is a rather more challenging problem. Classically, the formation of Laves phases has been thought to be determined by the requirements of sphere packing.[16] If we require that both A-A and B-B

contacts are formed, we arrive at an ideal radius ratio of $R_A/R_B = 1.225$ for the formation of a Laves phase. The effective size ratio deduced from the interatomic potentials of the pure metals (or equivalently from their Goldschimdt radii as described above) is $R_{Ca}/R_{Al} = 1.40$, $R_{Ca}/R_{Mg} = 1.28$, and $R_{Ca}/R_{Li} = 1.26$. Now contrary to what has to be expected from these size ratios, both $CaAl_2$ and $CaMg_2$ are very stable, congruently melting compounds with large negative enthalpies of formation, while $CaLi_2$ decomposes peritectically at a relatively low temperature.[21] The riddle is easily solved if we consider the interatomic potentials appropriate for the composition of a Laves phase. The effective size ratios deduced from the correct pair potentials are $R_{Ca}/R_{Al} = 1.15$, $R_{Ca}/R_{Mg} = 1.21$, $R_{Ca}/R_{Li} = 1.37$, in striking agreement with the observed stability of the compounds. The situation may be illustrated in form of a Pearson nearest-neighbor diagram plotting the reduced strain parameter $(D_A - d_{AA})/D_B$ against the size ratio $D_A/D_B = R_A/R_B$ ($D_i = 2R_i$ is the atomic diameter, d_{ij} is the interatomic distance). If the R_i are taken to be the Goldschmidt radii, the points for the observed phases are distributed along a line given by "Simon's rule"[39]

$$(D_A - d_{AA})/D_B = \alpha(R_A/R_B + n) - n\,, \tag{3}$$

where α is a geometrical constant and n indicates the stoichiometry of a general AB_n compound. This rule, whose validity is now established for a wide class of stoichiometric AB_n compounds, may be rewritten in the form of a simple law for the interatomic distances

$$d_{ij} = F_{ij}(R_A + nR_B)\,. \tag{4}$$

The F_{ij} are structure-dependent geometrical constants, for the AB_2 Laves phases $F_{AA} = 0.740$, $F_{AB} = 0.708$, $F_{BB} = 0.604$. Thus, Simon's rule expresses the additivity of the interatomic distances for stoichiometric intermetallic compounds. Deviations from the law are found in the case of

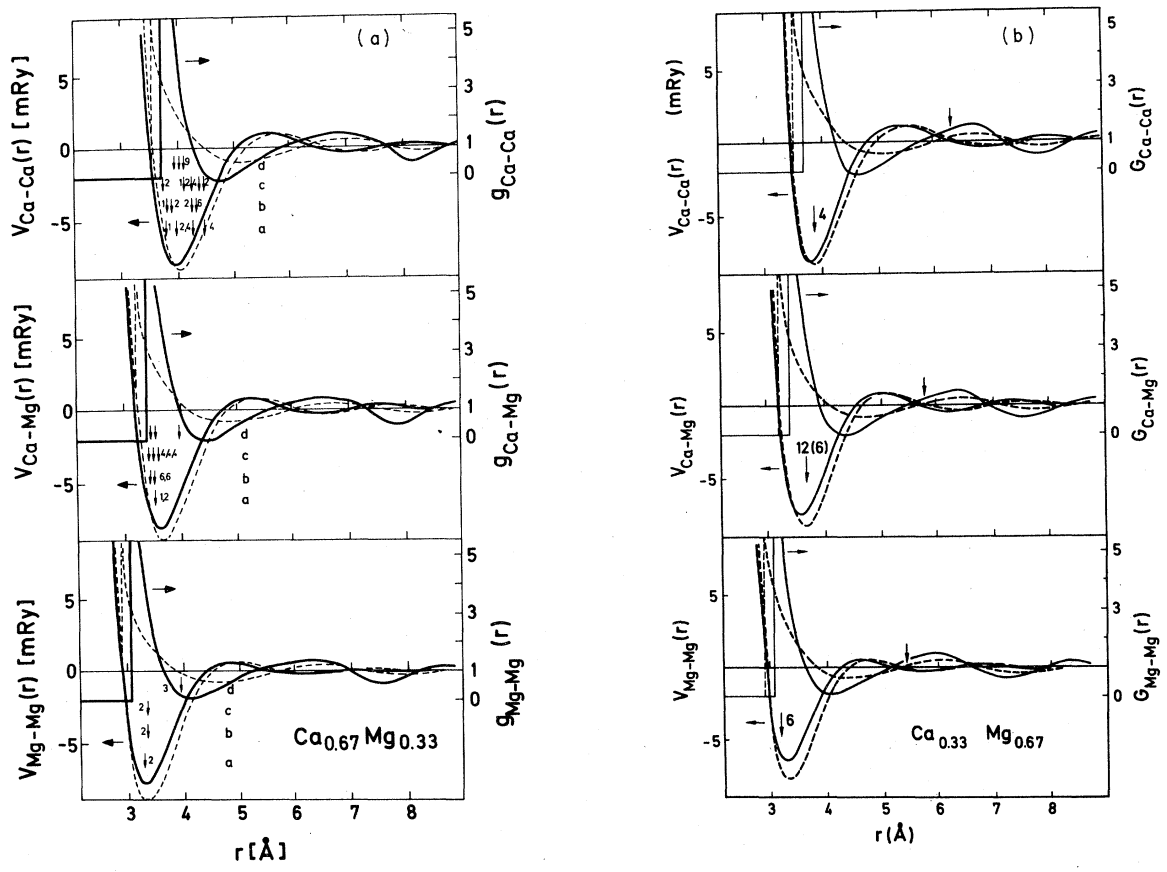

FIG. 3. Interatomic pair potentials $V_{ij}(r)$ and partial pair distribution functions $g_{ij}(r)$ for $Ca_{0.67}Mg_{0.33}$ (a) and $Ca_{0.33}Mg_{0.67}$ (b) in the glassy (bold lines, $T = 25$ °C) and in the liquid (broken lines, $T = 900$ °C) states. The vertical arrows indicate the interatomic distances in different hypothetical crystalline structures (a) and in the Laves phase ($MgZn_2$ type) lattice (b). The numbers given are the coordination numbers.

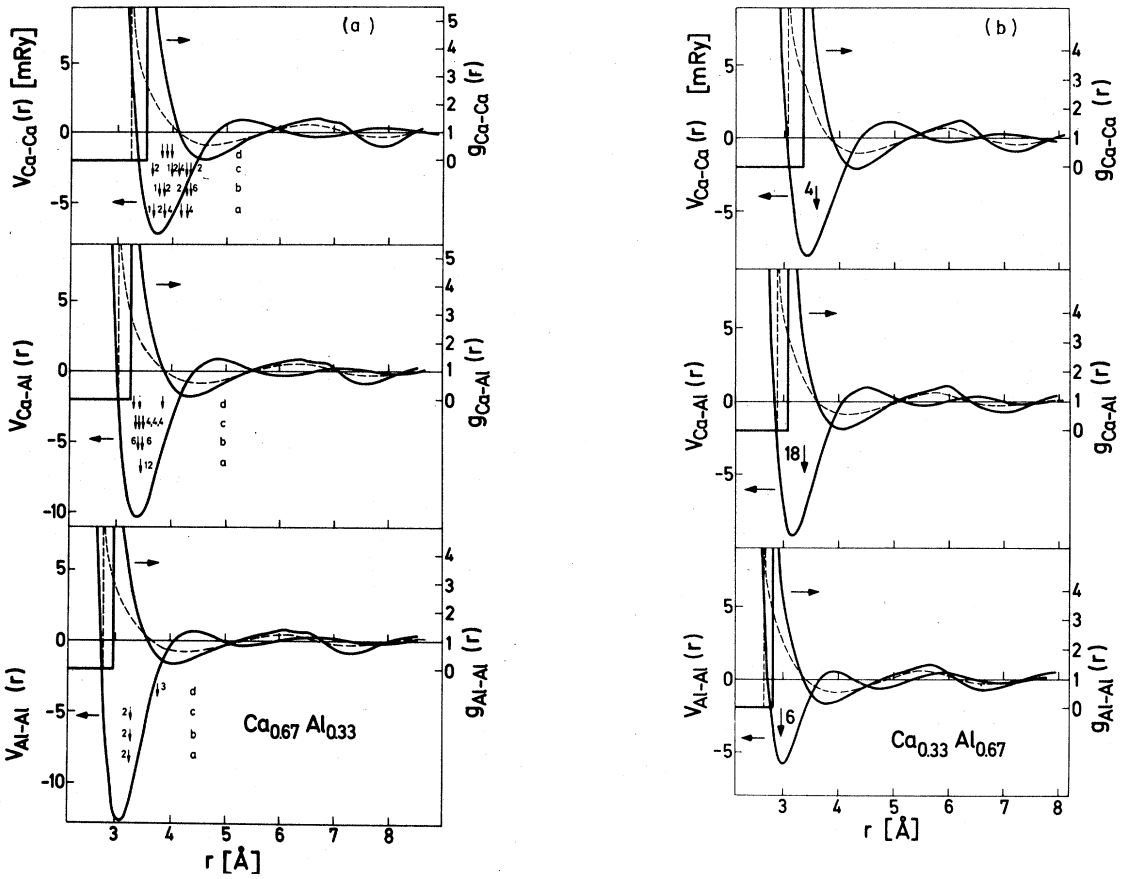

FIG. 4. Interatomic pair potentials $V_{ij}(r)$ and partial pair distribution functions $g_{ij}(r)$ for $Ca_{0.67}Al_{0.33}$ (a) and $Ca_{0.33}Al_{0.33}$ (b) alloys (cf. Fig. 3).

strong chemical bonding (large electronegativity difference) between the components. Simon's law is the counterpart of Vegard's law for mixed crystal, which predicts the additivity of the atomic volumes. The alloys considered here obey Simon's law quite well (Fig. 7). However, Simon's law does not predict a strain-free configuration. For larger size ratios, the contacts between the larger atoms appear to be appreciably compressed. Now, if we plot the nearest-neighbor diagram in terms of the effective atomic diameters in the alloy, the points representing the phases are shifted along the line described by Simon's law; those of the stable phases are now between the lines of strain-free contacts. This demonstrates that the formation of a Laves phase is governed by the tendency to form as many strain-free bonds as possible. This is illustrated in Figs. 3(a) to 5. The interatomic distances coincide very well with the minima in the interatomic potentials. Thus the physical principle for the bonding in Laves phases consists in a lowering of the electronic energy by packing as many atoms as possible into the minima of the pair interactions. The theory allows going one step further and differentiating between the different stacking variants of the Laves phases. In Table II we show the calculated energy differences between the cubic ($MgCu_2$ type) and the hexagonal ($MgZn_2$ and $MgNi_2$ types) Laves phases. In agreement with experiment, $MgZn_2$, $CaMg_2$, and $CaLi_2$ are predicted to be hexagonal ($MgZn_2$ type) and $CaAl_2$ is predicted to be cubic. This is an important test of our theory since the structural energy differences are the result of a close cancellation between electrostatic terms (which always prefer a cubic arrangement) and band-structure terms. Since the nearest-neighbor configuration is identical for all three structures, the success of the structure calculation tells us that our effective pair potentials are very realistic even for larger distances. In our treatment of the alkali-metal Laves phases[33] we have shown that the free (i.e., not determined by space group symmetry) parameters of the hexagonal Laves-phase structures may be calculated by minimizing the free energy in the configuration

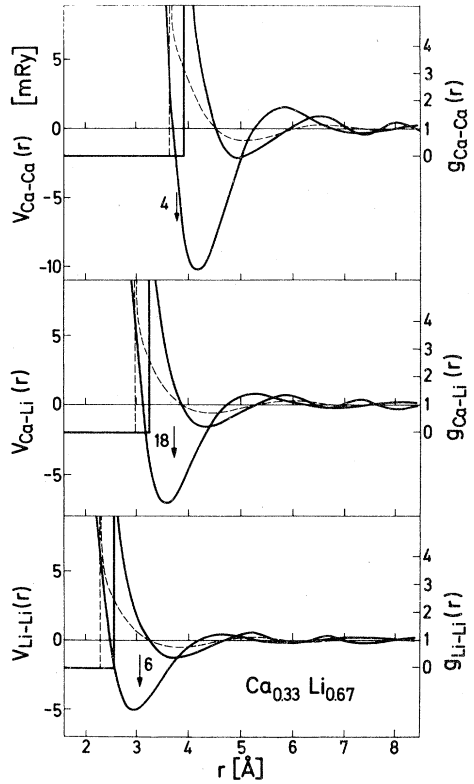

FIG. 5. Interatomic pair potentials $V_{ij}(r)$ and partial pair distribution functions $g_{ij}(r)$ for a $Ca_{0.33}Li_{0.67}$ alloy (cf. Fig. 3). The arrows indicate the interatomic distances in the $CaLi_2$ ($MgZn_2$ type) Laves phase.

space of the atomic positions. A similarly successful calculation has been performed for the compounds considered here. Both the electrostatic and the band-structure forces prefer strongly distorted, highly anisotropic atomic arrangements and the observed highly isotropic structure is the result of a very delicate forcebalance. This is important since it shows that our theory is accurate enough to explain the structure on a local microscopic level.

We have also calculated the thermochemical data for the alloys, e.g., the enthalpy of formation $\Delta H(CaMg_2) = -3.6$ Kcal/g-at. [expt. $\Delta H(CaMg_2) = -3.2$Kcal/g-at.[51]] and the volume of formation $\Delta\Omega(CaMg_2) = -9.2\%$ [expt. $\Delta\Omega(CaMg_2) = -5.6\%$[21]]. For the heterovalent alloys the calculation of ΔH is complicated by the fact that the electronic effects described above required a reconsideration of the structure-independent first-order contribution to the binding energy. This will be described in a subsequent publication.[40]

Our pair-potential argument is not restricted to Laves phases, but may be extended to more complicated intermetallic phases. A first example was the explanation of the K_7Cs_6 structure.[33] Figure 6 shows some preliminary results for the Ca-Zn system: it is demonstrated that the interatomic distances of the $CaZn_2$ ($CeCu_2$ type), $CaZn_5$ ($CaCu_5$ type), $CaZn_{11}$ ($BaCd_{11}$ type), and $CaZn_{13}$ ($NaZn_{13}$ type) compounds fit very well into the minima of the interatomic potentials (though it must be admitted that the correlation is not completely ideal for Zn-Zn neighbors—our calculation overestimates the radius of the Zn atom by about 0.06 Å, cf. Sec. III, possibly because of the neglect of *s-d* hybridization effects). A complete calculation of the thermochemical parameters of this system is underway and we are quite optimistic that we will be able to explain the relative stability of these compounds.

A unifying feature of most of the crystal structures considered here is their coordination polyhedra (CN). The smaller majority atoms have CN12 icosahedral coordination for the Laves, μ, and δ phases, not or partially not icosahedral for the $CaCu_5$, $BaCd_{11}$, and $NaZn_{13}$ structures. The CN12 polyhedra are linked by larger interpenetrating Frank-Kasper polyhedra (CN14, CN15, CN16) for the first group of structures, and by even larger polyhedra (CN18, CN20, CN22) for the latter structures.[37]

B. Mixed crystals

Glass formation is usually restricted to systems with a very low solid solubility. From our pair-potential picture it is immediately evident that due to the size difference a disordered arrangement of the ions on any possible lattice is energetically very unfavorable. We calculate large positive enthalpies ΔH and slightly positive volumes $\Delta\Omega$ of formation for mixed crystals in all the systems considered. An example of our results for hcp Ca-Mg mixed crystals is shown in Fig. 8. (The calculated structures for the pure metals are hcp for Mg and fcc for Ca. The calculated energy differences between the fcc and hcp polymorphs of Ca are extremely small. The hcp mixed crystal is lower in energy for up to 80 at.%Ca; for larger Ca contents the fcc mixed crystal is energetically more favorable, but the ΔH for the two structures are almost indistinguishable on the scale of our figure.)

C. Intermetallic compounds with compositions close to the composition of the glass

The formation of a metallic glass clearly requires that the possible intermetallic compounds with a composition falling in or near to the glass-forming region have a higher or at least only

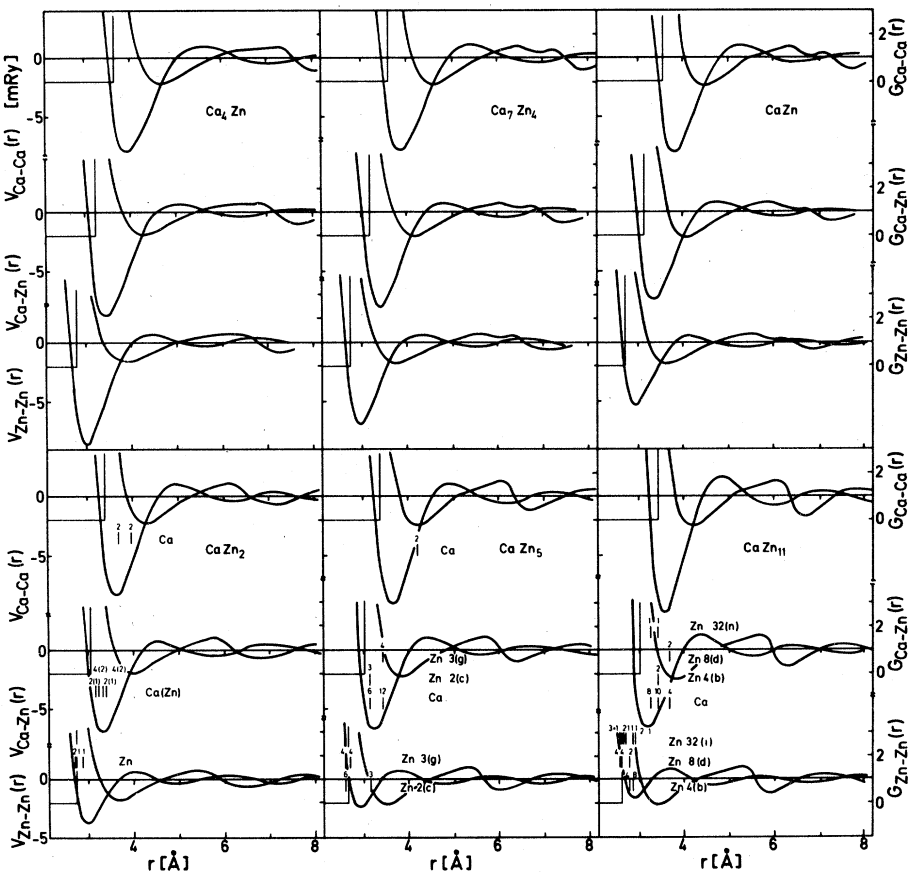

FIG. 6. Interatomic pair potentials $V_{ij}(r)$ and partial pair distribution functions $g_{ij}(r)$ for the supercooled liquid ($\approx$ glassy) state at $T = 25$ °C for the Ca-Zn system. The vertical bars demonstrate the interatomic distances and the coordination in the crystalline $CaZn_2$ ($CeCu_2$ type), $CaZn_5$ ($CaCu_5$ type), and $CaZn_{11}$ ($BaCd_{11}$ type) compounds. The notation for the atomic positions is that of the International Tables for X-ray Crystallography.

slightly lower free enthalpy than the glass itself (cf. Sec. I). Only a few glass-forming systems of group (b) form stable intermetallic compounds in the glass-forming region. Their structures, as well as those of the metastable crystalline compounds formed during the recrystallization process, are usually extremely complex and have not been resolved. A noticeable example is found in the Mg-Cu system: $MgCu_2$ is the prototype of a cubic Laves phase; Mg_2Cu has an orthorhombic structure. It is not very stable and decomposes at the eutectic temperature. The glass-forming region includes the composition Mg_2Cu. On annealing, the glass undergoes a glass transition and then crystallizes in the stable Mg_2Cu structure.[41]

TABLE II. Structural energy differences (relative to the stable structure) between the cubic ($MgCu_2$ type) and the two hexagonal ($MgZn_2$ and $MgNi_2$ types) Laves-phase structures.

Compound	ΔE (in cal/g-at.) $MgCu_2$	$MgZn_2$	$MgNi_2$
$MgZn_2$	220	0	1660
$CaLi_2$	470	0	1460
$CaMg_2$	25	0	560
$CaAl_2$	0	250	1600

Another example is found in the Pd-Zr and Cu-Zr systems. In our classification, they are limiting cases between groups (b) and (c)—this is justified from the structural evidence and from the fact that the *d* bands of Pd and Cu are already filled. Here the glass-forming region includes compounds Zr_2Cu and Zr_2Pd with the $MoSi_2$ crystal structure.

We shall now discuss the relative stability of hypothetical Mg_2Zn, Ca_2Mg, and Ca_2Al compounds with different possible crystal structures. The Mg_2Cu lattice, the closely related Mg_2Ni and $CuAl_2$ structures, the $MoSi_2$ lattice, and the re-

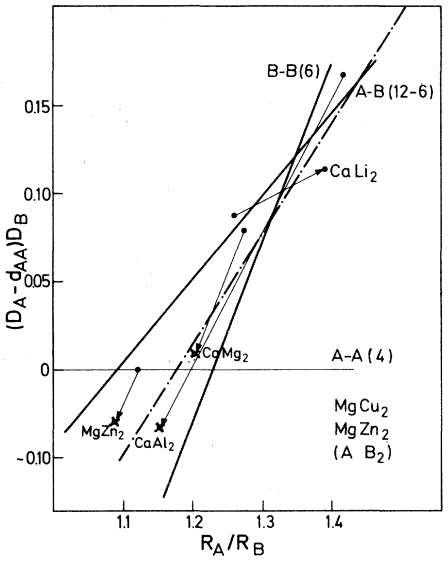

FIG. 7. Nearest-neighbor diagram (after Pearson, Ref. 37) for the Laves phases: D_i is the atomic diameter, R_i the atomic radius, d_{ij} the interatomic distance. The dot-dashed line represents Simon's rule [Eq. (3)]. Dots D_i and R_i as for the pure metals, crosses as deduced from the interatomic pair potentials in the alloys. The arrows show the importance of the renormalization of the size ratio and the strain parameter by charge-transfer and screening effects.

lated AlB_2 and $TiNi_2$ structures will be examined. These structures have been selected on the basis of radius-ratio considerations. In Figs. 3(a) and 4(a) we compare the interatomic distances of hypothetical Ca_2Mg and Ca_2Al compounds with the $CuAl_2$, Mg_2Cu, Mg_2Ni, and the $TiNi_2$ structures with the corresponding interatomic potentials. The distances are calculated according to Simon's rule [Eq. (4)], taking the atomic radii R_{min} as determined for the pure metals. In all cases the electronic effects discussed above (substitution

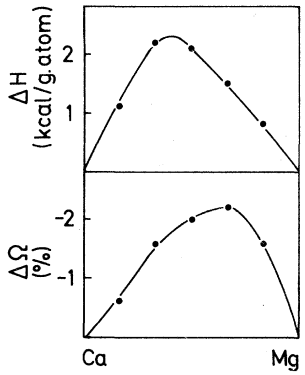

FIG. 8. Enthalpy ΔH and volume $\Delta\Omega$ of formation of a hypothetical hexagonal close-packed solid solution of Ca and Mg.

of R_{min} for the pure metals by the corresponding R_{min} for the alloy) yield a reduction of the strain parameters for most bonds. For the AlB_2, $MoSi_2$, and $TiNi_2$ structures there is no energetically favorable interrelation between distances and potentials. The coordination is energetically very unfavorable at least for some neighbors [only the case of the $TiNi_2$ lattice is shown explicitly in Figs. 3(a) and 4(a); the other two lattices have even higher energies]. It is clear that such structures with a rather anisotropic coordination cannot be stabilized by central pair potentials alone. On the other side, the interatomic distances of the $CuAl_2$, Mg_2Cu and Mg_2Ni lattices fit rather well into the minima of the pair potentials. We have estimated the relative configurational energies of the crystalline and amorphous phases in a very simple way by summing the pair interactions over the nearest-neighbor coordination shells only [Eqs. (1) and (2), for the pair-distribution functions of the amorphous phases, cf. Sec. V]. Our estimate predicts that the most stable crystalline structures are Mg_2Ni for Ca_2Al, and Mg_2Cu for Ca_2Mg and Mg_2Zn, the structural energy differences between the three lattices being of the order $\Delta E \sim 1200$ cal/g-at. However, the energy predicted for the glassy phase is nearly the same: ΔE relative to the most stable crystalline compound is $\Delta E \approx -280$ cal/g-at. for a-Ca_2Al, $\Delta E \approx 100$ cal/g-at. for a-Ca_2Mg, and $\Delta E \approx 200$ cal/g-at. for a-Mg_2Zn. To test the reliability of our estimate, we compare the estimated ΔE [a-$CaMg_2$-$CaMg_2$ (Laves phase)] ≈ 1500 cal/g-at. with the result of the exact calculation $\Delta E = 2000$ cal/g-at. and find a very reasonable agreement. Considering that the disordered phase has a higher entropy of formation we find that, in agreement with Turnbull's conjecture,[13] the amorphous alloys have a lower free energy than any single crystalline phase considered here.

The reason for the relatively low stability of the crystalline compounds is easy to explain. The average CN is 13.33 in the $CuAl_2$, Mg_2Cu, and Mg_2Ni lattices, it is the same as the average CN of the Laves phases. However, in contrast to the highly isotropic (i.e., all the bonds of one species have the same bond length) coordination in the Laves phases, the coordination is now quite anisotropic [cf. Figs. 3(a) and 4(a)]. This reduces the possibility of finding an energetically favorable arrangement in terms of pair potentials. Furthermore, though the number of A-A and A-B contacts is larger in the crystalline than in the amorphous A_2B compounds (cf. also Table III and Sec. V), the number of B-B neighbors is much smaller. A detailed comparison shows that while the energy of the A-A interactions is approximately the same

TABLE III. The numbers of nearest-neighbor correlations in amorphous and crystalline alloys.

	Origin	Amorphous				Crystalline			
A_xB_{1-x}	atom	A	B	total	average	A	B	total	average
$Mg_{70}Zn_{30}$ [a]	Mg	8.7	3.7	12.4	12.2				
	Zn	8.6	3.2	11.8					
$Mg_{70}Zn_{30}$ [b]	Mg	8.6	3.7	12.3	12.2				
	Zn	8.6	3.3	11.9					
$Ca_{67}Mg_{33}$ [b]	Ca	8.1	3.8	11.9	11.5	11	4	15	13.3 [c]
	Mg	7.6	3.2	10.8		8	2	10	
$Ca_{33}Mg_{67}$ [b]	Ca	5.2	8.7	13.9	12.3	4	12	16	13.3 [d]
	Mg	4.3	7.2	11.5		6	6	12	
$Ca_{67}Al_{33}$ [b]	Ca	8.3	3.7	12.1	11.6	11	4	15	13.3 [c]
	Al	7.5	3.3	10.8		8	2	10	
$Nb_{50}Ni_{50}$ [e]	Nb	5.2	5.9	11.1	11.8	7	8	15	13.4 [f]
	Ni	5.9	6.5	12.4		6.9	5.1	12	

[a] Calculated form the cluster PDF.
[b] Calculated from the variational hard-sphere PDF.
[c] The nearest-neighbor coordination numbers are the same for the $CuAl_2$, Mg_2Cu, and Mg_2Ni structures.
[d] Laves phase.
[e] After Chen and Waseda, Ref. 63.
[f] Average coordination number for the μ-phase Nb_6Ni_7.

in the crystalline and in the amorphous states, the A-B interactions prefer the crystalline and the B-B interactions the amorphous structure. Since, due to electronic screening effects (cf. Fig. 2), the B-B interactions are very strong in the alloy, this last contribution dominates.

IV. LIQUID ALLOYS

The combined application of pseudopotential and thermodynamic perturbation theories enables one to calculate the thermodynamic and structural properties of simple liquid metals and alloys from a quantum-mechanical basis. The pseudopotentials theory allows formulation of the internal energy in terms of the effective pair potentials (or energy–wave-number characteristics) and the partial pair-distribution functions (or partial structure factors).[23,24] Closed-form expressions for the structure factors[46] and the thermodynamic quantities of hard-sphere mixtures are furnished by Percus-Yevick theory.[42–44] Both theories are linked by a variational technique based on the Gibbs-Bogolyubov inequality.[45] This inequality states that if the Hamiltonian of a given system is regarded as the Hamiltonian of a reference system plus a perturbation, the free energy of the system will always be lower than that of the reference system plus the expectation value of the perturbation (calculated with the structure factors of the reference system). Our reference is that of a mixture of hard spheres, the perturbation is the deviation of our pair potentials from a hard-sphere behavior, and the hard-sphere diameters will be chosen to minimize the free energy. The resulting hard-sphere diameters σ_A, σ_B obey very well the relation[46–48]

$$V_{ij}(\sigma_{ij}) - V_{ij}^{\min} = \tfrac{3}{2}k_BT, \quad i,j = A,B, \tag{5}$$

i.e., the difference between the pair potential at σ_{ij} [with $\sigma_{AB} = \frac{1}{2}(\sigma_A + \sigma_B)$, the potentials are additive] and it's minimum value is just equal to the mean kinetic energy of free particles. The obvious meaning of Eq. (6) is that the hard-sphere diameters are the average collision-distances. Furthermore it shows that they are determined by the short-range part of the potentials only, i.e., by the depth of the attractive minimum and the steepness of the repulsive part. Equation (5) is also accurate enough to serve for an approximate determination of the hard-sphere diameters. Details of the application of the Gibbs-Bogolyubov technique have been described elsewhere,[26] so only the final results will be presented here.

The method yields both the structure and the thermodynamic quantities. In Fig. 9 we compare the theoretical structure factor and the pair distribution function for liquid Ca with the experimental results of Waseda *et al.*[49] The agreement is quite impressive and tells us that the repulsive part of the Ca-pair potential is sufficiently hard-core-like to make our approach realistic. Similar results for other metals can be found in an earlier paper.[26] No experimental investigation

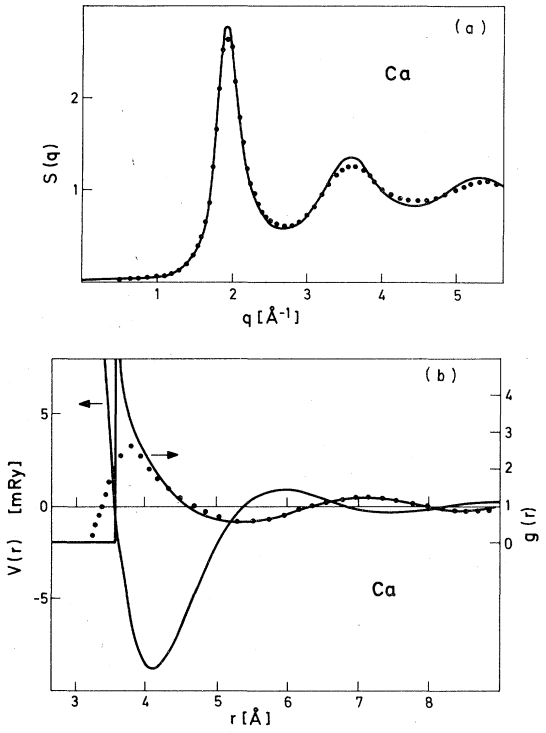

FIG. 9. Static structure factor $S(q)$ (a) and pair distribution function $g(r)$ (b) for liquid Ca at $T = 850$ °C. Solid line theory: the dots represent the experimental results of Waseda *et al.* (Ref. 49).

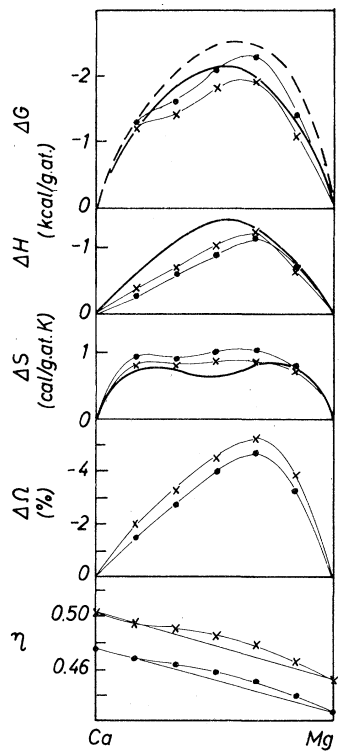

FIG. 10. Free enthalpy ΔG, enthalpy ΔH, entropy ΔS, and volume $\Delta\Omega$ of formation, and the packing fraction η for liquid Ca-Mg alloys. The points and crosses represent the calculated values at $T = 900$ °C (●) and $T = 700$ °C (×). The continuous line represents the experimental results of Sommer *et al.* ($T = 737$ °C, Ref. 50), and the broken line the ΔG (for $T = 923$ °C) quoted by Hultgren *et al.* (Ref. 51).

of the liquid structure of one of the alloys considered here is known.

A comprehensive calculation of the thermodynamic properties over the entire concentration range has been performed for the Ca-Mg system, because this is the only alloy for which complete experimental data are available.[50,51] Our results for the free enthalpy ΔG, the enthalpy ΔH, the entropy ΔS, and the volume $\Delta\Omega$ of formation are shown in Fig. 10. Taking into account that we are calculating extremely small energy differences, the agreement with experiment is exceedingly good. The asymmetry in the ΔG curves (the maximum of the theoretical curve is at ~65 at.% Mg; expt. at ~54 at.% Mg) shows that there is no particular stabilization of the melt at the eutectic composition (≈27 at.% Mg). It is not necessary to assume the formation of $CaMg_2$ associates[50] in the melt to explain the concentration dependence of ΔG. The asymetry in ΔG results from the asymmetry in the dense random packing of two different kinds of spheres. For purely geometrical reasons it is easier to achieve a high packing density (yielding a lower energy) at a majority concentration of the smaller atoms than at a majority concentration of the larger atoms. This is evidenced by the concentration dependence of the volume of formation and of the packing density (cf. Fig. 10). The change of the mean atomic radius $\bar{r}$ is very small over the entire concentration range $\Delta r \lesssim 1\%$. This suggests the possibility to extend Simon's rule of additive interatomic distances to disordered close-packed systems. There is a slight inflection in the ΔG curve at ~33 at.% Mg, which of course should not exist in a completely miscible system. So at this stage it is certainly a spurious effect due to the limited accuracy of our calculations. Nonetheless there is a possibility that this a remnant of a thermal effect found in the glassy state.[14] We will come back to this point in Secs. V and VI.

Again it is very instructive to study the interrelation between the pair potentials and the interatomic distances as given by the partial pair distribution functions (Figs. 3 to 6). From Eq. (2) it is clear that if the minima of the pair potentials coincide with the maxima of the corresponding partial pair distribution functions, the integrand

$V(r)[g(r)-1]$ will be negative over the largest part of the integration range, yielding a very low configurational energy. We see that this "constructive interference" between $V(r)$ and $g(r)$ is realized over the entire range of Ca-Mg alloys. We note that the physical mechanism for the stabilization of the liquid alloy is identical to that for the stabilization of the Laves phase.

The conditions for this type of interference occurring depend on the size ratio and on the compatibility of the wavelength of the oscillations in $V(r)$ and $g(r)$. Asymptotically, they go as

$$V_{ij}(r) \rightarrow \cos(2k_F r)/r^3 \tag{6}$$

and

$$[g_{ij}(r)-1] \rightarrow \sin(Q_{ij} r)/r\,, \tag{7}$$

where k_F is the Fermi wave vector and Q_{ij} is the wave vector where the partial structure factor $S_{ij}(q)$ has it's first maximum. The Q_{ij} are related to the hard-sphere diameters by a phenomenological relation due to Blétry[52]:

$$Q_{ij} = \frac{1}{\sigma_{ij}}\ 7.64 - 4.32\ \frac{\bar{\sigma}}{\sigma_{ij}} - 1 \tag{8}$$

with the average sphere diameter $\bar{\sigma} = c_A\sigma_A + c_B\sigma_B$. At the first look, Eqs. (6) and (7) point to the Nagel-Tauc rule $Q_{ij} = 2k_F$ and suggest an interpretation of this rule in terms of a pair-potential argument, as proposed by Beck and Oberle.[53] Upon closer inspection we see that due to the different size of the components ($Q_{AA} \neq Q_{AB} \neq Q_{BB}$), a constructive interference of all three $g_{ij}(r)$ (which do not oscillate in phase) with the corresponding $V_{ij}(r)$ (which oscillate in phase) is impossible in the asymptotic region. Anyway, this is not very important, since the amplitude of the oscillations is strongly damped. The matching between the interatomic distances and the minima of the potentials is more important for short and intermediate distances, where $V_{ij}(r)$ (especially that of the minority atoms) deviates quite substantially from its asymptotic form. In this region, the existence of an energetically favorable interrelation between $V_{ij}(r)$ and $g_{ij}(r)$ is a more complicated function of the atomic radii [which determine the wavelength of the oscillations in $g_{ij}(r)$ and the initial phases of both $g_{ij}(r)$ and $V_{ij}(r)$], the valence electron concentration (VEC) [which determines k_F and hence the wavelength of the oscillations in $V_{ij}(r)$], and of the electronegativity difference (which determines the renormalization of the atomic radii through electronic bonding effects).

V. AMORPHOUS ALLOYS–METALLIC GLASSES

The first realistic approach to the structure of metallic glasses was the Polk hypothesis,[2,54] which assumes that quenched amorphous alloys can be described by the Bernal dense random packing of hard spheres (DRPHS) model.[55] Von Heimendahl[56] and Barker *et al.*[57] independently made the important step of relaxing the Bernal model structure under assumed pair potentials of a Lennard-Jones type. Very recently, von Heimendahl introduced two essential improvements in the relaxation process[28]: (i) The interactions between the atoms are described by the pseudopotential-derived pair potentials calculated by the present author and (ii) periodic boundary conditions. The last point allows elimination of surface effects, such as unphysical density fluctuations which arise when finite clusters are used to simulate bulk properties. The use of realistic pair potentials accounts for the two-component nature of the metallic glass and for the chemical processes in the formation of the alloy. It constitutes an important improvement over Lennard-Jones-type potentials, especially for higher than nearest-neighbor interactions.

The starting point of the relaxation calculation was a cluster of 800 atoms inside a regular rhombic dodecahedron, taken from the center of Finney's big DRPHS model.[58] The pair potentials are used to calculate the total force $\vec{F}(\vec{r}_1)$ on the atom situated at $\vec{r}_1$. While all other atoms are kept fixed at their positions, one can calculate the displacement $\delta\vec{r}_1$ necessary to move the atom into a force-free position $\vec{r}_1' = \vec{r}_1 + \delta\vec{r}_1$. In the relaxation procedure the $\delta\vec{r}_1$ of all atoms are calculated and stored. Then the new positions $\vec{r}_1''$ are calculated by adding a certain fraction of $\delta\vec{r}_1$ to $\vec{r}_1$. Starting from the new positions, the whole procedure is repeated until the latest set of $\delta\vec{r}_1$ is negligible. This relaxation algorithm is essentially equivalent to the steepest-descent algorithm described by Hoare.[59]

The result of von Heimendahl's calculation for the partial pair-distribution functions and the partial structure factors of the $Mg_{0.7}Zn_{0.3}$ glass are shown in Figs. 11 and 12. They show the structure in the second peak which is usually observed in amorphous systems the $S_{ij}(q)$ may be used to calculate the intensity for the elastic scattering of neutrons and x rays. In Figs. 13(a) and 13(b) the theoretical results are compared with the experiments of Rudin.[60] For the neutron scattering the agreement with experiment is quite excellent, apart form a slighly underestimated splitting of the second peak. The main peak in the x ray scattering intensity $I(Q)$ lies at $Q_p = 2.56$ Å^{-1} (theory); respectively, $Q_p = 2.68$ Å^{-1} (experiment), again with a quite good overall agreement. If we try to interpret these results, we have to consider that the x-ray scattering

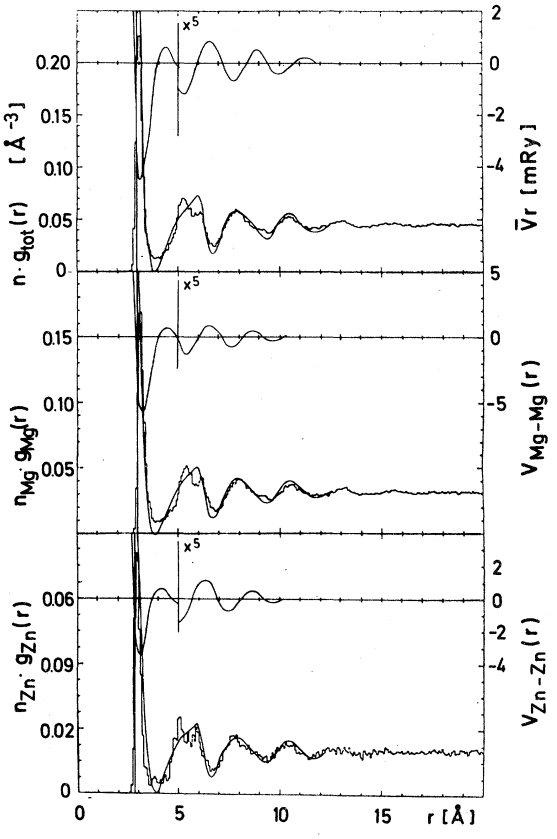

FIG. 11. Total and partial pair distribution functions $g_{ij}(r)$ for the $Mg_{0.7}Zn_{0.3}$ glass. The histogram shows the result of the cluster-relaxation calculation, the continuous line the result of the thermodynamic variational technique ($T = 25$ °C). The average and the partial interatomic potentials $V_{ij}(r)$ are shown in the inset (right-hand scale).

form factor of Zn is much bigger than that of Mg, ~75% of $I(Q)$ originates from the Zn atoms. Hence we can conclude that our Mg potential seems to be very accurate, while our Zn potential yields Zn-Zn distances which are approximately 0.12 Å larger than found in the experiment. This agrees with our prior estimate (Secs. II. and III A).

In Fig. 11 we can again compare the potentials and the pair distribution functions. It is no longer surprising that there is again a one-to-one correspondence between the minima in the V_{ij}'s and the maxima of the g_{ij}'s. Thus, the glass is stabilized by the same close-packing mechanism than the Laves phase and the liquid alloy.

It is worthwhile to pursue this last correlation somewhat further. Nearly every review article on metallic glasses starts with the comparison of the structure factors of the liquid and the glass. The intermediate state—the supercooled liquid—is generally not accessible to experiment. There is no such problem for a theoretical investigation. We can apply our Gibbs-Bogolyubov variational technique to room temperature. For a supercooled Mg_7Zn_3 alloy at $T = 25$ °C we get $\sigma_{Zn} = 2.76$ Å, $\sigma_{Mg} = 2.96$ Å, corresponding to an average packing density of hard spheres of $\eta = 0.62$. The variationally determined hard-sphere pair-distribution functions (PDF's) and structure factors compare very well with the result of the cluster-relaxation calculation (Figs. 10 and 11), the position, height, and shape of the oscillations are very well reproduced.[61] This result is important for two reasons: (i) It demonstrates that except for some degree of short-range order (which is manifest in the splitting of the second peak), the structure of the glass is identical to that of the supercooled liquid and (ii) it allows the study of the interrelation between the PDF's and the pair potentials without the expense of a full cluster-relaxation calculation. In Figs. 3 to 6 we display this relationship for the systems Ca-Mg, Ca-Al, Ca-Li (with the σ_{ij}'s calculated using the full variational technique) and Ca-Zn [with σ_{ij} estimated using Eq. (5)] both in the liquid and supercooled liquid (≈amorphous) states. For the Ca-Mg, Ca-Zn, and Ca-Al systems, the potentials and the PDF's are very well "in phase" over the hole range of nonnegligible interionic forces. For Ca-Mg and Ca-Zn this is true for all concentrations, while for Ca-Al, the PDF's and $V_{ij}(r)$ are well in phase on the Ca-rich side, but as the Al content is increased, the maxima of the PDF's move out of the minima of the potentials for second and higher neighbors. For the Ca-Li system we have $Q_{Li\text{-}Ca} \approx 2k_F$, so one would expect a similarly favorable PDF-V_{ij} relation. However, due to the large size difference ($\sigma_{Li}/\sigma_{Ca} = 0.65$), the second peak in the PDF is split and the second neighbors are shifted to energetically less favorable distances, this correlates with the fact that the constitution diagram of Ca-Li is of a peritectic type and that there is no glass formation in this system.

It is interesting to compare our results with some recent experimental information on T-T glasses. In Table III the theoretical coordination numbers (CN) for our Mg-Zn, Ca-Mg, and Ca-Al glasses, calculated from $g_{ij}(r)$ according to the prescription of Sadoc and Dixmier,[62] are listed together with the results for a Nb-Ni glass, derived from the experimental $g_{ij}(r)$ of Chen and Waseda.[63] Of course the HS model does not show any preferred coordinations, but we see that this is also the case for the cluster calculation and for the experimental CN. The total CN is nearly constant ≈12 and there are only very small differences in the coordination of the larger and

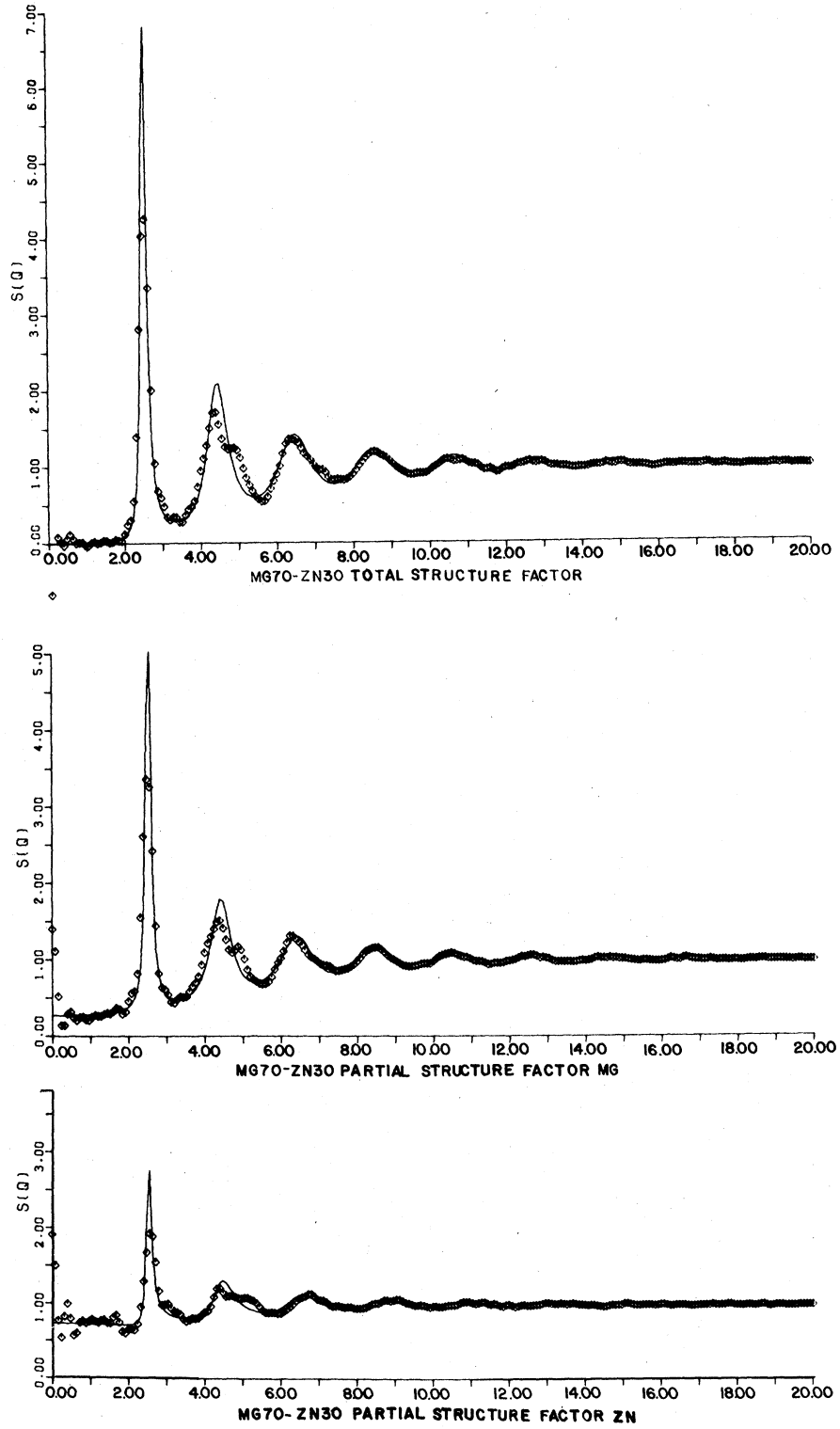

FIG. 12. Total and partial structure factors $S_{ij}(q)$ for the $Mg_{0.7}Zn_{0.3}$ glass. The squares represent the result of the cluster-relaxation calculation, the continous line the hard-sphere structure factors calculated via the thermodynamic variational technique. Q is given in units of $Å^{-1}$.

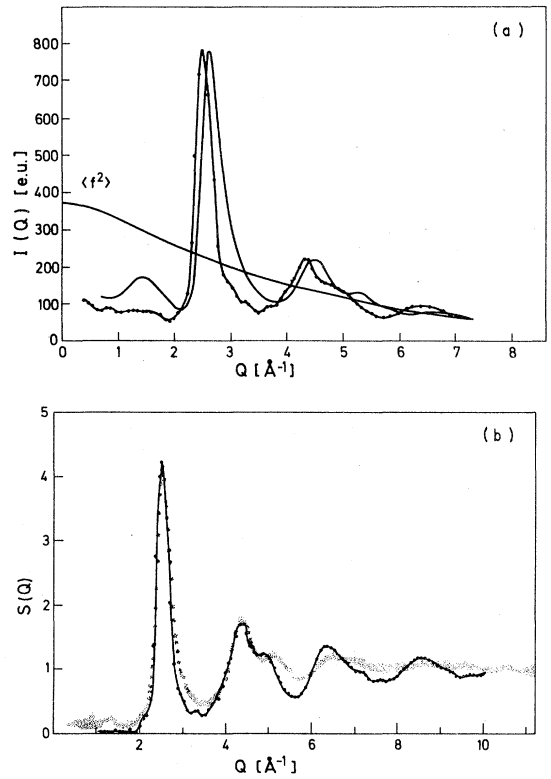

FIG. 13. (a) Elastic coherent x-ray scattering intensity $I(Q)$ for the $Mg_{0.7}Zn_{0.3}$ glass. The points represent the result of the cluster-relaxation calculation, with the x-ray form factors f_{Mg} and f_{Zn} calculated by pseudopotential theory. The continuous line is the measured scattering intensity. (b) Interference function $S(Q)$ for coherent elastic neutron scattering by a glassy $Mg_{0.7}Zn_{0.3}$ alloy. The dots joined by a full line shows the result of the cluster-relaxation calculation. The shaded area represents the spread of the experimental points The experimental data have been kindly communicated by H. Rudin prior to publication (Ref. 60).

smaller atoms. This is in marked contrast to T-M glasses where unlike-atom pairs are strongly preferred, but appears to be a common fact of all group (b) and (c) (cf. Table I) glasses.

The concentration dependence of the interatomic distances demonstrates another common aspect. The interatomic distances (for simplicity we take the HS diameters σ_{ij}) in amorphous Ca-Mg, Ca-Al, Cu-Zr, and Nb-Ni alloys are shown in Fig. 14. We see that the contraction of the A-A and A-B distances (where A stands for the component with the lower electronegativity) is common to many metallic glasses. In Sec. II we have shown that this contraction arises from a charge transfer due to orthogonalization and screening effects. Similar charge transfers, possibly involving d electrons may be expected for T-T glasses.

Finally, the Gibbs-Bogolyubov method permits

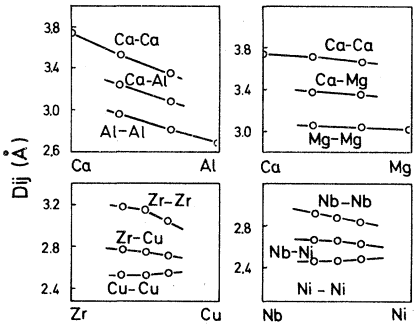

FIG. 14. The average nearest-neighbor distances D_{ij} in amorphous Ca-Mg and Ca-Al alloys (theory) and Nb-Ni and Cu-Zr alloys (experimental, after Chen and Waseda, Ref. 63).

at least an estimate of the thermodynamic properties of a metallic glass. The results for Ca-Mg at room temperature are shown in Fig. 15. They are similar to the results for the liquid alloy: ΔH and $\Delta\Omega$ are asymetric due to packing effects, ΔS deviates substantially from the ideal (parabolic) form. The main point is that there is no minimum of ΔG in the glass-forming region. The formation of a glass is determined by several concurring factors. It is interesting that the ΔG curve is concave at ~35%Mg. If this is not a spurious result, it means that the supercooled liquid tends to phase separate into liquids with ~15% and ~50%Mg. St. Amand and Giessen[15] note that "in the Ca-Mg system, heating may result in phase separation

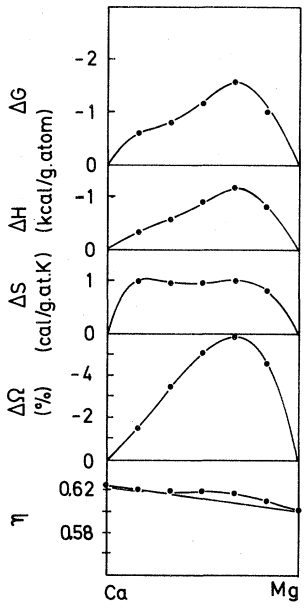

FIG. 15. Free enthalpy ΔG, enthalpy ΔH, entropy ΔS, and volume $\Delta\Omega$ of formation, and packing fraction η of supercooled liquid ($\approx$ amorphous) Ca-Mg alloys at $T = 25$ °C (relative to the supercooled pure metals).

of a single glass into two glasses." This point deserves further investigation.

The predicted volume of formation should not be directly compared to the experimental density of the glass. As pointed out by Chen and Jackson,[64] the specific volume of a metallic glass depends on it's thermal history. The thermal expansion coefficient changes discontinuously at the glass transition temperature, which in turn depends on the cooling rate. Thus our calculated density is rather an upper bound than the realistic value.

VI. PHASE DIAGRAM AND GLASS FORMATION

We can combine the results of Secs. III–V to derive the phase diagram and the essential criteria for the glass formation. However, there is still a "missing link" in our theory: Our results for the crystalline phases refer to $T = 0$ °K; we have to calculate their thermodynamic properties. For the pure metals this constitutes, at least in principle, no difficulty. We know that our pseudopotentials yield very accurate phonon spectra,[31] thus we can directly use this information to calculate the vibrational energy and entropy in a quasiharmonic approximation, or even add anharmonic corrections. This method has been used to treat temperature-induced martensitic transitions.[31,65] Another possibility would be to use a Gibbs-Bogolyubov variational method, the reference system being now a solid with a Debye[66] or an Einstein[67] spectrum. Here we shall content ourselves with an even simpler estimate. We calculate the Debye temperature from the phonon dispersion relations: Mg $\theta_D = 390$ °K [expt. $\theta_D(T = 0\ ^\circ\mathrm{K}) = 396\ ^\circ\mathrm{K}$]; Ca $\theta_D = 235$ °K [expt. $\theta_D(T = 0\ ^\circ\mathrm{K}) = 230\ ^\circ\mathrm{K}$].[68] Taking a temperature-independent θ_D, and computing the free energy in a quasiharmonic approximation, we calculate the melting points of the pure metals: $T_M(\mathrm{Ca}) \sim 1400$ °C, [expt. $T_M(\mathrm{Ca}) = 850$ °C]; $T_M(\mathrm{Mg}) \sim 800$ °C, [expt. $T_M(\mathrm{Mg}) = 650$ °C] with a reasonable accuracy. In order to account in a global way for anharmonic effects, we adjust the energy difference between the solid and the liquid in such a way that our simple estimate yields the correct melting temperature. The required adjustment is quite small, only 8%(Mg) and 15% (Ca) of $F_s(T_M) - F_s(T = 0)$. For the mixed crystal we assume an ideal entropy of formation ΔS; ΔS for the Laves phase is taken from experiment ($\Delta S_{\mathrm{CaMg_2}} = -0.2$ cal/g-at. K),[51] both assumptions having no influence on the following.

We have now collected all necessary ingredients for constructing ΔG diagrams as a function of temperature. The limits of stability of the different phases are determined by a common-tangent construction [Fig. 16(a)]. In this way we derive a

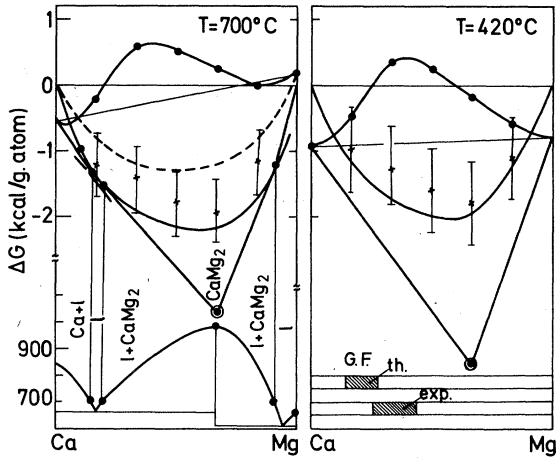

FIG. 16. Free enthalpy ΔG of formation (relative to the pure liquid, respectively supercooled liquid metals) of Ca-Mg alloys at $T = 700$ °C and $T = 420$ °C (i.e , close to the recrystallization temperature): ●—solid solution, ×—liquid (respectively, supercooled liquid) solution, ○—Laves phase. The error bars represent the estimated uncertainty, the full line is a tentative interpolation. The common-tangent construction for the determination of the phase diagram and of the glass-forming range is indicated (cf. text).

fully realistic phase diagram [cf. Fig. 1(a)]. The melting temperature of the Laves phase is somewhat overestimated, since the theoretical ΔG is lower than the experimental one for the Laves phase and vice versa for the liquid alloy. In view of the extreme difficulty of the problem, this is certainly a success. The picture demonstrates very clearly in which manner the eutectic composition is determined by the relative magnitude of G for the liquid and crystalline phases.

A similar plot may be constructed for a temperature below the lowest eutectic [Fig. 16(b)]. We see that there is a limited concentration range in which ΔG of the supercooled liquid is very close to the straight line representing the ($\mathrm{Ca} + \mathrm{CaMg_2}$) two-phase mixture (in interpolating the ΔG values, we ignore for the moment the inflection at ~33% Mg, cf. the discussion in the previous section). If the system is constrained against phase separation (this is now a kinetic condition) glass formation will occur with great ease.

These diagrams show the way in which both the destabilization of possible crystalline phases and the stabilization of the disordered (liquid or amorphous) phase cooperate in the formation of metallic glasses. The width of the glass-forming range is limited by the stoichiometry of the stable intermetallic compounds. If the maximum stability occurs at a higher concentration of the smaller B atoms (this is the case for a higher size ratio R_A/R_B, e.g., in the Ca-Zn system),

the diagrams of Fig. 16 are somewhat more asymmetric. The ΔG curve of the amorphous alloy will be parallel to the two-phase line over a broad concentration range. This explains the correlation between the width of the glass-forming region and the component size ratio noted by St. Amand and Giessen.[15]

The energetics of phase stabilization and destabilization may be understood in terms of our pseudopotential approach. The geometrical principle underlying all stable phases, both ordered and disordered, is tetrahedral close packing. At minority concentration of the larger A atoms, this leads to structures formed by interpenetrating coordination polyhedra: icosahedra around the smaller B atoms, larger Frank-Kasper and Friauf polyhedra around the larger A atoms. At a majority concentration of the larger atoms, we have again a coordination in the form of triangulated coordination shells, typically CN = 15 around the larger and CN = 10 around the smaller atoms ($CuAl_2$, $CuMg_2$, and $NiMg_2$ structures[37]). The CN for A-A contacts is now higher than that corresponding to a statistical distribution (cf. Table III), at the expense of a reduced number of B-B contacts. This yields a relatively high configurational energy, even though the interatomic distances fit tolerably well into the minima of the pair potentials. An icosahedral coordination

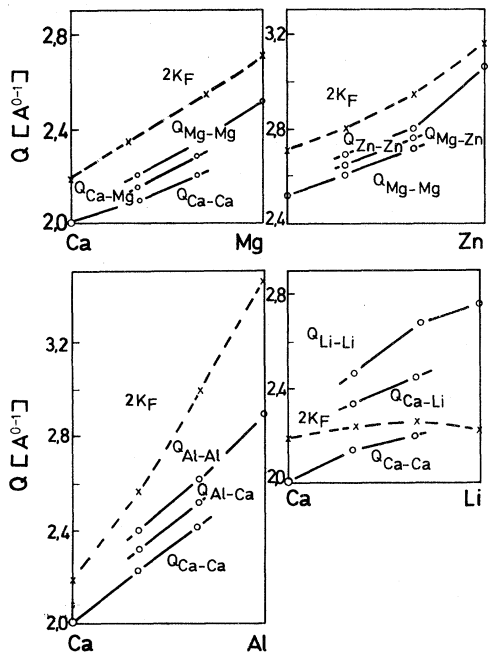

FIG. 17. Positions Q_{ij} of the main peak in the partial structure factors $S_{ij}(Q)$ and Fermi wave vector k_F versus concentration for several amorphous alloys.

of the small B atoms would be energetically preferable, but seems to be incompatible with the requirement of crystal periodicity.

For the metallic glasses we have approximately CN = 12 for both kinds of atoms, the partial coordination corresponds to a random distribution of A-A, A-B, and B-B bonds. Thus we could speculate, following Briant and Burton,[69] on icosahedral coordination polyhedra as the constituting element of the structure of metallic glasses. They have pointed out that 13 atoms in an icosahedral packing form 42 nearest-neighbor contacts, six more than in a closest crystalline packing. Thus an icosahedral arrangement will be preferred for attractive nearest-neighbor interactions. Our pair potentials are attractive not only for nearest, but also for second- and third-nearest neighbors. This leads very naturally to the larger icosahedral units discussed by various authors.[59,69,70] An analysis of the relaxed cluster in terms of the local coordination will be needed to clarify this point. The occurrence of icosahedral units with their fivefold symmetry is also suggested as a possible mechanism for lowering the entropy of the glass without the onset of crystallization.[59]

It is evident that the cornerstone of our theory is the existence of an oscillation effective pair potential which is attractive for all neighbors within the range of nonnegligible interatomic forces. We turn now to the necessary conditions for such a "constructive interference" between pair potentials and pair-distribution functions. As we have already mentioned in Sec. IV, the most obvious, but not satisfying, interpretation is a Nagel-Tauc type rule[3] $Q_p \cong Q_{ij} \cong 2k_F$. Let us consider this rule once more. Figure 18 shows that the alloy which fulfills this condition most closely is Ca-Li, the only one which does not form a glass. It is very easy to establish a long list of counterexamples: Li-Mg, Li-Al, Al-Mg, etc. The reason is that the Nagel-Tauc rule emphasizes the VEC and neglects all other alloy-chemical factors such as size ratio and electronegativity.

Our theory manifests the similarity of the chemical bonding in crystalline, amorphous, and liquid alloys. The relative importance of the alloy-chemical factors is the classical one:

(i) size-ratio, (ii) strong chemical bonding (charge transfer and screening), (iii) valence-electron concentration. Our treatment of the Ca-Al glass shows very clearly the way in which (a) a high component size ratio (in terms of the pure metal radii), (b) a relatively large electronegativity difference (strong bonding), and (c) a high average alloy valence all contribute to the stability of metallic glasses. The empirical validity of

these correlations has been demonstrated by Giessen and co-workers.[11,15] The most important factor is an *effective* size ratio allowing for an icosahedral close packing ($R_A/R_B \sim 1.1$ to 1.3). The VEC is also important, but since (counting only s-p electrons) it can vary only from 1 to 4, it is evidently not a very sharp criterion.

Technically, our method is restricted to simple-metal glasses. The comparison of our results with results on T-T glasses, however, suggests that many aspects are common to all metalloid-free glasses. This is corroborated by recent theoretical work on the interatomic forces in transition metals[71] that demonstrate the usefulness of the pair-potential concept at least for close-packed d-band metals.

ACKNOWLEDGMENTS

The work presented in this paper was stimulated by very fruitful cooperation of Dr. L. von Heimendahl. Enlightening discussions with Professor H. J. Güntherodt, Professor V. Heine, Professor B. C. Giessen, Professor H. Rudin, Dr. F. Sommer, and Dr. M. Fischer are gratefully acknowledged. The author is indebted to Professor Rudin and Dr. F. Sommer for communicating unpublished material. He thanks Professor H. Bilz and Professor O. Hittmair for their support. The TU Vienna part of this work was sponsored by the "Fonds zur Förderung der wissenschaftlichen Forschung in Österreich" under Contract No. 3857.

---

*Present address.

[1]W. Klement, R. H. Willens, and P. Duwez, Nature 187, 809 (1960).

[2]C. H. Bennett, D. E. Polk, and D. Turnbull, Acta Metall. 19, 1259 (1971).

[3]S. R. Nagel and J. Tauc, Phys. Rev. Lett. 35, 380 (1975).

[4]L. Meisel and P. J. Cote, Phys. Rev. B 15, 2970 (1977).

[5]K. Froböse and J. Jäckle, J. Phys. F 7, 2331 (1977).

[6]S. R. Nagel, Phys. Rev. B 16, 1694 (1977).

[7]P. Oelhafen, M. Liard, H. J. Güntherodt, K. Berresheim, and H. D. Polaschegg, Solid State Commun. 30, 641 (1979).

[8]J. D. Riley, L. Ley, J. Azoulay, and K. Terakura, Phys. Rev. B 20, 776 (1979).

[9]U. Mizutani, K. T. Hartwig, T. B. Massalski, and R. N. Hopper, Phys. Rev. Lett. 41, 661 (1978).

[10]E. Esposito, H. Ehrenreich and C. D. Gelatt, Phys. Rev. B 18, 3913 (1978).

[11]B. C. Giessen, J. Hong, L. Kabacoff, D. E. Polk, R. Raman, and R. St. Amand, in *Proceedings of the Third International Conference on Rapidly Quenched Metals, Brighton*, 1978, edited by B. Cantor (The Metals Society, London, 1978).

[12]H. S Chen, Acta Metall. 24, 153 (1976); H. S. Chen, Mat. Sci. Eng. 23, 151 (1976).

[13]D. Turnbull, *Solidification* (American Society for Metals, Metals Park, Ohio, 1971), p. 1.

[14]D. E. Polk and B. C. Giessen, *Metallic Glasses* (American Society for Metals, Metals Park, Ohio, 1978), p. 1.

[15]B. C. Giessen, Workshop on Dense Random Packing, Liège, 1978 (unpublished); R. St. Amand and B. C. Giessen, Scr. Metall. 12, 1021 (1978).

[16]F. C. Frank and J. S. Kasper, Acta Crystallogr. 11, 184 (1958); 12, 483 (1959).

[17]For recent reviews, see, e.g., H. J. Güntherodt, in *Advances in Solid State Physics*, edited by H. J. Treusch (Vieweg, Braunschweig, 1977), Vol. XVII, p. 25; S. Takayama, J. Mat. Sci. 11, 164 (1976).

[18]A. Calka, M. Madhava, D. E. Polk, B. C. Giessen, H. Matya, and J. VanderSande, Scr. Metall. 11, 65 (1977); K. Hülse and B. Predel, J. Less-Common Met. 63, 45 (1979); F. Sommer, G. Duddek, and B. Predel, Z. Metallkun. 69, 587 (1978).

[19]L. E. Tanner and R. Ray, Scr. Metall. 11, 783 (1977); L. E. Tanner and B. C. Giessen, Met. Trans. 9A, 67 (1978).

[20]G. S. Cargill, in *Thin Film Phenomena—Interfaces and Interactions*, edited by J. E. Baglin and J. M. Poate (The Electrochemical Society, Princeton, 1978), p. 221.

[21]M. Hansen, *Constitution of Binary Alloys* (McGraw-Hill, New York, 1958); R. P. Elliott, *Constitution of Binary Alloys*, 1st suppl. (McGraw-Hill, New York, 1965); F. A. Shunk, *Constitution of Binary Alloys*, 2nd suppl. (McGraw-Hill, New York, 1969); W. G. Moffat, *Binary Phase Diagram Handbook* (General Electric, Schenectady, 1976).

[22]R. Ray, B. C. Giessen, and N. J. Grant, Scr. Metall. 2, 357 (1968); J. Vetek, J. VanderSande, and N. J. Grant, Acta Metall. 23, 165 (1975); B. C. Giessen, M. Madhava, and D. E. Polk, Mat. Sci. Eng. 23, 145 (1976).

[23]W. A. Harrison, *Pseudopotentials in the Theory of Metals* (Benjamin, New York, 1966).

[24]V. Heine and D. Weaire, in *Solid State Physics, Advances in Research and Applications*, edited by H. Ehrenreich, F. Seitz, and D. Turnbull (Academic, New York, 1971), Vol. 24, p. 247.

[25]W. H. Young, in *Proceedings of the Third International Conference on Liquid Metals, Bristol*, 1976, edited by R. Evans and D. A. Greenwood (The Institute of Physics, London and Bristol, 1977), Conf. Series, Vol. 30, p. 7.

[26]J. Hafner, Phys. Rev. A 16, 351 (1977).

[27]J. Weeks, D. Chandler, and H. C. Andersen, J. Chem. Phys. 54, 5237 (1971).

[28]L. von Heimendahl, J. Phys. F 9, 161 (1979).

[29]J. Hafner and L. von Heimendahl, Phys. Rev. Lett. 42, 386 (1979).

[30]J. Hafner, J. Phys. F 6, 1243 (1976).

[31]For any details concerning the construction of the

crystal potential, see J. Hafner, Z. Physik B22, 351 (1975); B24, 41 (1976); J. Hafner and H. Eschrig, Phys. Status Solidi B 72, 179 (1975).
[32]P. Vashishta and K. S. Singwi, Phys. Rev. B 2, 875 (1972).
[33]J. Hafner, Phys. Rev. B 15, 617 (1977).
[34]H. Ruppersberg and W. Speicher, Z. Naturforschung 31a, 47 (1976); W. Biltz and F. Weibke, Z. Anorg. Allgem. Chem. 223, 321 (1935).
[35]L. Pauling, *The Nature of the Chemical Bond* (Cornell Univ. Press, Ithaca, 1952).
[36]J. Hafner and F. Sommer, CALPHAD 1, 350 (1977).
[37]For a description of the different structure types mentioned in this article we refer to W. B. Pearson, *The Crystal Chemistry and Physics of Metals and Alloys* (Wiley-Interscience, New York, 1972), and to the Structure Reports.
[38]A. Simon, W. Brämer, B. Hillenköter, and H. J. Kullmann, Z. Anorg. Allgem. Chem. 419, 253 (1976).
[39]A. Simon, in Proceedings of the Third European Crystallogr. Meeting, Zürich 1976, p. 335.
[40]J. Hafner (unpublished).
[41]F. Sommer (private communication).
[42]E. Thiele, J. Chem. Phys. 39, 474 (1963).
[43]M. S. Wertheim, Phys. Rev. Lett. 10, 321 (1963); J. Math. Phys. 8, 927 (1964).
[44]N. F. Carnahan and K. E. Starling, J. Chem. Phys. 51, 635 (1969); G. A. Mansoori, N. F. Carnahan, K. E. Starling, and T. W. Leland, J. Chem. Phys. 54, 1523 (1971). This version of the hard-sphere equation of state has been used in our calculations.
[45]A. Isihara, J. Phys. A 1, 539 (1968).
[46]N. W. Ashcroft and D. C. Langreth, Phys. Rev. 156, 685 (1967).
[47]J. Hafner, in *Proceedings of the Third International Conference on Liquid Metals, Bristol*, 1976, edited by R. Evans and D. A. Greenwood (The Institute of Physics, London and Bristol, 1977), Vol. 30, p. 109.
[48]F. Igloi, Phys. Status Solidi B 92, K85 (1979).
[49]Y. Waseda, K. Yokoyama, and K. Suzuki, Phil. Mag. 30, 1195 (1974).
[50]F. Sommer, B. Predel, and D. Assmann, Z. Metallk. 68, 347 (1977), and private communication.
[51]R. Hultgren, P. D. Desai, D. T. Hawkins, M. Gleiser, K. K. Kelley, and D. D. Wagmans, *Selected Values of the Thermodynamic Properties of Binary Alloys* (American Society of Metals, Metals Park, Ohio, 1973).
[52]J. Blétry, Z. Naturforschung 33a, 327 (1978).
[53]H. Beck and R. Oberle, in *Proceedings of the Third International Conference on Rapidly Quenched Metals, Brighton*, 1978, edited by B. Cantor (The Metals Society, London, 1978), Vol. I, p. 416.
[54]D. E. Polk, Scr. Metall. 4, 117 (1970).
[55]J. D. Bernal, Proc. R. Soc. London A280, 299 (1964).
[56]L. von Heimendahl, J. Phys. F 5, L141 (1975).
[57]J. A. Barker, J. L. Finney, and M. R. Hoare, Nature 257, 120 (1975).
[58]J. L. Finney, Proc. R. Soc. London A319, 479 (1970).
[59]See, e.g., M. Hoare, J. Non-Cryst. Solids 31, 157 (1978).
[60]H. Rudin (unpublished report and private communication).
[61]That a two-component hard-sphere model calculated in the mean-spherical approximation might be a suitable approach to the structure of metallic glasses has already been suggested by J. D. Weeks, Phil. Mag. 35, 1345 (1977).
[62]J. F. Sadoc and J. Dixmier, Mat. Sci. Eng. 23, 187 (1976).
[63]H. S. Chen and Y. Waseda, Phys. Status Solidi B 51, 593 (1979).
[64]H. S. Chen and K. A. Jackson, *Metallic Glasses*, edited by J. J. Gilman and H. J. Leamy (American Society for Metals, Metals Park, Ohio, 1978), p. 74.
[65]G. K. Straub and D. C. Wallace, Phys. Rev. B 3, 1234 (1971); R. Pynn and I. Ebbsjö, J. Phys. F 1, 744 (1971).
[66]D. Stroud and N. W. Ashcroft, Phys. Rev. B 5, 371 (1971).
[67]M. Hasegawa and W. H. Young, J. Phys. F 7, 2271 (1977).
[68]K. A. Gschneider, *Solid State Physics, Advances in Research and Applications*, edited by H. Ehrenreich, F. Seitz, and D. Turnbull (Academic, New York, 1964), Vol. 16.
[69]C. L. Briant and J. J. Burton, Phys. Status Solidi B 85, 393 (1978).
[70]J. Farges, B. Raoult, and G. Torchet, J. Chem. Phys. 59, 3454 (1973).
[71]C. C. Matthai, P. J. Grount, and N. H. March, Int. J. Quant. Chem. S12, 443 (1978).